

Interior design of a two-dimensional semiclassical black hole: Quantum transition across the singularity

Dana Levanony and Amos Ori

Department of Physics, Technion, Haifa 32000, Israel

(Dated: October 30, 2018)

We study the internal structure of a two-dimensional dilatonic evaporating black hole, based on the CGHS model. At the semiclassical level, a (weak) spacelike singularity was previously found to develop inside the black hole. We employ here a simplified quantum formulation of spacetime dynamics in the neighborhood of this singularity, using a minisuperspace-like approach. Quantum evolution is found to be regular and well-defined at the semiclassical singularity. A well-localized initial wave-packet propagating towards the singularity bounces off the latter and retains its well-localized form. Our simplified quantum treatment thus suggests that spacetime may extend semiclassically beyond the singularity, and also signifies the specific extension.

PACS numbers:

I. INTRODUCTION

The inevitable occurrence of spacetime singularities inside black holes (BHs) constitutes one of the greatest challenges in understanding the final fate of gravitational collapse. A spacetime singularity is typically a region in spacetime where the curvature blows up. The presence of spacetime singularities inside BHs has been established by several theorems [1], and is also demonstrated by numerous examples of exact BH solutions.

Such curvature singularities are often regarded in the literature (at least formally) as the boundary of spacetime. It is not obvious that this assertion is fully justified from the physical view-point (especially in the case of weak singularities; see below). This formal point of view is nevertheless pragmatic, because even if spacetime does physically extend beyond the singularity, in most cases it is unclear what this extension is: The singularity makes the mathematical extension ambiguous, as the field equations become ill-defined there. One may hope, however, that once the full theory of Quantum Gravity is formulated, it will somehow resolve the spacetime singularities and thereby clarify how physics extends beyond them.

The remarkable revelation of Hawking radiation [2] and black-hole evaporation brought new and intense interest into black-hole structure, and particularly into the associated information puzzle. The latter appears to be intimately related to the presence of a singularity inside the BH: As long as the hypersurface of singularity is treated as a boundary of spacetime, all bits of information which encounter this hypersurface are quite inevitably "destroyed" there. For this reason one may naturally hope that the information puzzle will eventually be resolved by Quantum Gravity eliminating spacetime singularities.

Two decades ago Callan, Giddings, Harvey and Strominger (CGHS) [3] introduced a toy model for investigating the formation and evaporation of black holes. Their toy model consists of two-dimensional gravity coupled to a dilaton field. In this two-dimensional framework the renormalized stress-energy tensor $\hat{T}_{\alpha\beta}$ may be expressed

in a simple explicit form, for any prescribed background metric. This property makes the CGHS model a powerful tool for analyzing BH evaporation. At the classical level (ignoring the semiclassical corrections), one finds a one-parameter family of vacuum solutions, analogous to the Schwarzschild solution in four dimensions. Once the semiclassical effects are added, the BH emits a thermal Hawking radiation and evaporates.

Originally it was hoped that the CGHS model of BH formation and evaporation will be free of any singularity, which would make it an ideal model for addressing the information puzzle. However, Russo, Susskind and Thorlacius [4] soon demonstrated that a spacelike curvature singularity actually forms inside the semiclassical CGHS BH. This singularity was recently analyzed in some detail [5], based on the homogeneous approximation. Quite remarkably, the singularity turns out to be *weak* in Tipler's terminology [6] [7]. This means that extended physical objects arrive at the singular hypersurface intact (as opposed to a strong singularity where the object is totally torn apart). What diverges at the CGHS singularity is the *rate of change* of the metric and the dilaton (e.g. in terms of the proper time along a timelike geodesic). In other words, the dilaton and metric are continuous but non-smooth at the singularity.

Owing to the weakness of the semiclassical CGHS singularity, one may be tempted to assume that semiclassical spacetime will somehow extend beyond the singular hypersurface. This leads one to consider the issue of existence and uniqueness of solutions to the semiclassical CGHS field equations, in the spacetime region laying at the future side of the spacelike singularity—solutions which continuously match the data coming from the past side. It is not difficult to see that existence is not a problem, but uniqueness fails here because we had to give up on smoothness. In fact, there is an infinite set of such continuous semiclassical extensions beyond the singularity. Semiclassical theory alone thus fails to predict the correct extension—even if such an extension does exist in reality. One may hope, however, that a fully-quantized version of the CGHS model will address this problem

(e.g. by resolving the singularity). It should tell us if spacetime indeed extends semiclassically beyond the singularity, and if so—what the correct extension is.

Motivated primarily by the BH information puzzle, Ashtekar, Taveras and Varadarajan (ATV) [8] recently proposed a quantized version of the CGHS model. In their model (roughly speaking) the dilaton and the metric conformal factor are elevated to quantum fields defined on an \mathbb{R}^2 manifold. These quantum fields are represented by operators, within the Heisenberg picture. The field equations thus turn into a nonlinear system of operator partial differential equations, with initial data specified at past null infinity. A key question underlying this model is whether the quantum evolution, formulated in this way, retains its regularity at the (would-be) semiclassical singularity. It is conceivable that regularity is preserved at the quantum level, though this still needs to be shown. If regularity is indeed preserved, then in principle quantum evolution could be followed within this model all the way from the collapse to full evaporation. In particular this would clarify the state of the quantum fields accessible to an observer at future null infinity, thereby resolving the information puzzle. Unfortunately the nonlinear operator equations underlying the ATV model are extremely hard to solve. To overcome this difficulty, ATV introduced two useful approximates: Bootstrapping, which may be applied to the early stage of evaporation; and the mean-field approximation, which presumably holds near future null infinity.

In the ATV scenario, the singularity which was present in the semiclassical picture is now replaced by a region of strong quantum fluctuations. Quantum dynamics is presumably regular there, which allows for a well-defined evolution of (quantum) spacetime across this region. A priori there are several possibilities: (i) After a narrow strongly-fluctuating transition region (marking the locus of the semiclassical spacelike singularity), the fluctuations weaken and spacetime retains its semiclassical character; or, alternatively, (ii) quantum fluctuations never decline, and spacetime remains strongly-fluctuating in the entire causal future of the semiclassical singularity. Intermediate options are also possible: For example, spacetime may become semiclassical again only in the neighborhood of future null infinity.

Our main goal in this paper is to explore the quantum transition across the semiclassical spacelike singularity, and to reveal the nature of the spacetime region at the immediate neighborhood of this singularity. Particularly we would like to find out if spacetime indeed becomes semiclassical again after crossing the singularity [option (i) above], and if so—what is the semiclassical solution which takes place there. Unfortunately, none of the approximate solutions constructed by ATV apply to this portion of the manifold (and the operator field equations are extremely difficult to solve). In order to circumvent this difficulty, in this paper we shall apply one further simplification to the quantum ATV dynamics, and treat it at the "minisuperspace" level—that is, we shall ignore

all degrees of freedom associated with inhomogeneities.

Our motivation comes from the observation that the semiclassical dynamics inside a macroscopic evaporating CGHS BH—and in particular the approach to the spacelike singularity—may well be approximated (locally) by homogeneous solutions of the CGHS field equations (see discussion in [5]). In this sense the BH interior resembles an approximately-homogeneous cosmology, which is amenable to a quantum treatment at the minisuperspace level. Our quantization strategy thus proceeds as follows: (i) We employ the homogenous approximation for the BH interior already at the semiclassical level, erasing any reference to spatial dependence. Correspondingly we regard our variables (metric and dilaton) as mere time-dependent variables, rather than fields; (ii) We explore the leading-order asymptotic behavior of our variables on approaching the spacelike singularity. (iii) We derive an effective Hamiltonian which reproduces this leading-order dynamics near the singularity. [Note that stages (i-iii), which are implemented at the semiclassical level, were already carried out in Ref. [5].] (iv) We now quantize our variables, but we do this in a way one quantizes time-dependent variables (rather than fields). Thus, the dynamics is now represented by a time-dependent wave-function Ψ , and the effective Hamiltonian becomes a differential operator which determines the time evolution of Ψ via a Schrodinger-type equation.

A key objective of this paper is to explore the properties of this simplified quantum system. We first obtain the stationary eigenfunctions, construct from them a well-localized initial wave packet, and follow its time evolution after it hits the singularity.

Summary of main results - A key result in our analysis is that *the quantum evolution is regular and hence well-defined*. This is not a trivial result, since the Hamiltonian operator \hat{H} itself is in fact singular at the locus of the semiclassical singularity. Yet, all its eigenfunctions are perfectly regular there, yielding a unique regular quantum evolution across the semiclassical singularity.

Our initial conditions correspond to a well-localized wave packet which propagates towards the singularity. At this initial stage the wave packet follows a semiclassical orbit, as expected. As the wave packet approaches the singularity, it slightly spreads and develops numerous wiggles. Subsequently, the wave packet bounces off the singularity, and retains its original well-localized character. In this final stage, too, the wave packet is found to follow a semiclassical orbit—a particular member of the infinite set of possible (continuous) semiclassical solutions beyond the singularity. Thus, this quantum model determines the specific semiclassical extension which takes place to the future of the semiclassical singularity. The extension of the dilaton turns out to be (at the leading order near the singularity) a time-reflection of the evolution prior to the singularity. However, the extension of the other degree of freedom (the metric conformal factor) does not admit the same time-reflection symmetry.

Concluding, our quantum model suggests that in an evaporating CGHS BH, spacetime physics extends beyond the spacelike singularity by means of a well-defined semiclassical spacetime. It remains to explore the detailed structure of this new patch of spacetime. In this paper we only obtained its leading-order asymptotic behavior just beyond the singularity. The extension beyond leading order is discussed in sec. VII.

We must recall, however, that the quantum model considered here is a very simplified one. To obtain more firm and trustable results, one must resort to a fuller quantum-gravitational theory of spacetime dynamics.

The paper is organized as follows: In section II we briefly review the main results of the semiclassical analysis carried out in Ref. [5], which are relevant to the present work. In particular this includes the leading-order semiclassical asymptotic behavior near the singularity, and the corresponding effective Hamiltonian.

Section III describes our quantization procedure, and also presents the eigenfunctions of the stationary Schrodinger equation. Section IV will be devoted to the construction of a well-localized initial wave-packet, while Sec. V will discuss the time evolution of the wave packet and its properties as it hits the singularity and afterward. In Sec. VI we present the (leading-order) semiclassical extension of spacetime beyond the singularity, as determined from the orbit of the well-localized wave packet after it bounces off the singularity. Finally, Sec. VII is dedicated to discussion of our results and their significance.

Throughout this paper we use general-relativistic units $c = G = 1$.

II. BACKGROUND

In Ref. [5] we investigated the interior of a macroscopic evaporating CGHS BH, and particularly the singularity which develops inside the BH. Here we shall briefly outline the main results, and establish the notation relevant to the quantum analysis below.

A. The model and field equations

The semiclassical CGHS model [3] describes gravity in $1 + 1$ dimensions coupled to a dilaton ϕ . It also includes a cosmological constant λ^2 and a large number $N \gg 1$ of identical scalar matter fields f_i . We express the metric in double-null coordinates u, v , namely $ds^2 = -e^{2\rho} du dv$. The action is

$$\frac{1}{\pi} \int du dv [e^{-2\phi} (-2\rho_{,uv} + 4 \phi_{,u} \phi_{,v} - \lambda^2 e^{2\rho}) - \frac{1}{2} \times \sum_{i=1}^N f_{i,u} f_{i,v} + \frac{N}{12} \rho_{,u} \rho_{,v}]. \quad (1)$$

The last term represents the semiclassical correction. For notational simplicity we set $\lambda = 1$ [this choice amounts to a trivial shift $\rho \rightarrow \rho + \ln(\lambda)$].

For convenience we introduce new variables: $\tilde{R} \equiv e^{-2\phi}$ (which was denoted R in [5]) and $S \equiv 2(\rho - \phi)$. The evolution equations then read

$$\tilde{R}_{,uv} = -e^S - K \rho_{,uv}, \quad S_{,uv} = K \rho_{,uv} / \tilde{R}, \quad (2)$$

where $K \equiv N/12$, and $\rho = \frac{1}{2}(S - \ln \tilde{R})$ is to be substituted. The constraint equations are

$$\tilde{R}_{,ww} - \tilde{R}_{,w} S_{,w} + \hat{T}_{ww} = 0, \quad (3)$$

where w stands for either u or v , and \hat{T}_{ww} denotes the semiclassical energy fluxes (whose explicit form is not needed here). We have set here $f_i = 0$ (a trivial solution of the scalar field equation $f_{i,uv} = 0$), as we are dealing here with the evaporation of the BH rather than its formation.

It is useful to re-express the system of evolution equations (2) in its standard form, in which $\tilde{R}_{,uv}$ and $S_{,uv}$ are explicitly given in terms of lower-order derivatives:

$$\begin{aligned} \tilde{R}_{,uv} &= -e^S \frac{(2\tilde{R} - K)}{2(\tilde{R} - K)} - \tilde{R}_{,u} \tilde{R}_{,v} \frac{K}{2\tilde{R}(\tilde{R} - K)}, \\ S_{,uv} &= e^S \frac{K}{2\tilde{R}(\tilde{R} - K)} + \tilde{R}_{,u} \tilde{R}_{,v} \frac{K}{2\tilde{R}^2(\tilde{R} - K)}. \end{aligned} \quad (4)$$

This form makes it obvious that the evolution equations become singular at $\tilde{R} = K$ and $\tilde{R} = 0$.

B. homogenous set-up

In Ref. [5] it was established that the spacetime inside a macroscopic evaporating CGHS black hole is (locally) approximately homogeneous. Motivated by this observation, we shall restrict our attention to homogeneous solutions of the field equations. Namely, we consider solutions which only depend on $t \equiv v + u$. In the homogeneous framework the evolution equations (4) become

$$\ddot{\tilde{R}} = -e^S \frac{(2\tilde{R} - K)}{2(\tilde{R} - K)} - \dot{\tilde{R}}^2 \frac{K}{2\tilde{R}(\tilde{R} - K)}, \quad (5)$$

$$\ddot{S} = e^S \frac{K}{2\tilde{R}(\tilde{R} - K)} + \dot{\tilde{R}}^2 \frac{K}{2\tilde{R}^2(\tilde{R} - K)}, \quad (6)$$

where an over-dot denotes differentiation with respect to t . The constraint equations (3) now turn into a single equation

$$\ddot{\tilde{R}} - \dot{\tilde{R}} \dot{S} + \hat{T} = 0,$$

where $\hat{T} \equiv \hat{T}_{vv} = \hat{T}_{uu}$.

C. The $\tilde{R} = K$ Singularity

The semiclassical evolution equations are singular at $\tilde{R} = 0$ and $\dot{\tilde{R}} = K$. In a black-hole interior \tilde{R} decreases monotonically, starting from a macroscopic value ($\tilde{R} \gg K$) at the horizon. Therefore, of these two singular values, it is $\dot{\tilde{R}} = K$ which is first encountered. Since the evolution beyond this singularity is a priori unknown, it is not clear whether the semiclassical $\tilde{R} = 0$ singularity will ever be encountered. For this reason we concentrate here on the $\dot{\tilde{R}} = K$ singularity (which is *guaranteed* to develop).

As it turns out, this singularity is characterized by the divergence of $\dot{\tilde{R}}$ and \dot{S} , while \tilde{R} and S are finite. The evolution equations are dominated near the singularity by [5]

$$\ddot{\tilde{R}} = -\frac{\dot{\tilde{R}}^2}{2(\tilde{R} - K)}, \quad \ddot{S} = \frac{\dot{\tilde{R}}^2}{2K(\tilde{R} - K)}. \quad (7)$$

The general solution is

$$\tilde{R}(t) = K + B|t - t_0|^{\frac{2}{3}}, \quad (8)$$

$$S(t) = -\frac{B}{K}|t - t_0|^{\frac{2}{3}} + (t - t_0)B_2 + B_3. \quad (9)$$

It depends on four arbitrary parameters B, B_2, B_3, t_0 as required. We find that \tilde{R} and S are indeed continuous at $t = t_0$, but $\dot{\tilde{R}}$ and \dot{S} diverge as $|t - t_0|^{-1/3}$.

To simplify the description of the asymptotic behavior near $\dot{\tilde{R}} = K$ we re-define our variables as

$$R \equiv \tilde{R} - K, \quad Z \equiv \tilde{R} + KS.$$

The above near-singularity evolution equations then decouple and take the simple form

$$\ddot{R} = -\frac{\dot{R}^2}{2R}, \quad \ddot{Z} = 0. \quad (10)$$

D. Effective Hamiltonian for the near-singularity region

Next we construct an effective Hamiltonian which yields the leading-order asymptotic behavior near $\dot{\tilde{R}} = K$, with the aim of subsequently quantizing this dynamical system.

For the R -motion one finds the Hamiltonian [5]

$$H = \frac{P^2}{R} \quad (11)$$

(up to an arbitrary multiplicative constant), where P is the momentum conjugate to R . For Z we obviously have the free-particle Hamiltonian $H_Z = \frac{1}{2}P_Z^2$, where P_Z is the momentum conjugate to Z . The overall leading-order effective Hamiltonian is $H + H_Z$.

Note that the effective Hamiltonian (11) is independent of t , hence H must be conserved along any semiclassical solution $R(t)$. Indeed one finds that $\dot{R} = \partial H / \partial p = 2P/R$ and therefore Eq. (8) yields a constant H ,

$$H = \frac{R\dot{R}^2}{4} = \frac{B^3}{9}. \quad (12)$$

III. QUANTIZATION OF THE SYSTEM AND EIGEN-FUNCTIONS

We turn now to quantize our dynamical system, proceeding as outlined in Sec. I. Since the near-singularity dynamics of z is trivial, we shall focus here on the quantization of R (the trivial quantum evolution of z will be briefly addressed at the end of Sec. V). The dynamics of R is thus described by a wave-function $\Psi(R, t)$, which admits the usual probabilistic interpretation of Schrodinger theory. The wave function evolves in time according to the Schrodinger equation

$$i\hbar\partial_t\Psi = \hat{H}\Psi. \quad (13)$$

Here \hat{H} denotes the Hamiltonian operator, namely an operator version of the semiclassical Hamiltonian (11), in which P is replaced by the momentum operator $\hat{P} = -i\hbar\partial_R$.

Since \hat{P} is a differential operator, the ordering of \hat{P} and the factor $1/R$ matters, and different orderings may lead to different quantum theories. There are many possible orderings, and a priori it is not clear which is the "right" one. Here we choose the simplest symmetric ordering:

$$\hat{H} = \hat{P}\frac{1}{R}\hat{P} = -\hbar^2\partial_R\frac{1}{R}\partial_R. \quad (14)$$

In 1+1 dimensions, the combination $\hbar G/c^3$ turns out to be dimensionless (for any choice of length, time, and mass units). Since we have already chosen General-Relativistic units $c = G = 1$, the constant \hbar is dimensionless. In what follows we choose the value $\hbar = 1$. A different choice of \hbar will amount to a rescaling of the "Energy" parameter E (which we shortly introduce)—and correspondingly a rescaling of the time scale for quantum evolution. [12]

The system's eigenstates $\psi_E(R)$ are determined by the time-independent Schrodinger equation $\hat{H}\psi_E(R) = E\psi_E(R)$, namely

$$\left(\frac{d}{dR}\frac{1}{R}\frac{d}{dR}\right)\psi_E(R) = -E\psi_E(R). \quad (15)$$

The general solution of this equation is

$$\psi_E(R) = C_A A i'(-E^{1/3}R) + C_B B i'(-E^{1/3}R) \quad (16)$$

(for $E \neq 0$), where Ai and Bi respectively denote the Airy functions of the first and second kinds, the prime

denotes a derivative with respect to their argument, and C_A, C_B are arbitrary coefficients. [13]

Note that both functions $Ai(x)$ and $Bi(x)$ are real, and are analytic at $x = 0$. It is remarkable that unlike the semiclassical singularity at $R = 0$ — and despite the singular $1/R$ factor which explicitly appears in the Hamiltonian — all eigenfunctions $\psi_E(R)$ are absolutely regular at $R = 0$. This fact is crucial to our approach: It implies that a generic wave packet $\psi(R, t)$ propagating towards small R will not experience any singularity on approaching $R = 0$, hence it will admit a unique and well-defined evolution afterward.

We may only use eigenfunctions which are square-integrable. Note the far-zone asymptotic behavior of the Airy functions: For $x \gg 1$ we have

$$Ai(x) \approx \frac{1}{2\sqrt{\pi}x^{1/4}} \exp(-\frac{2}{3}x^{3/2}), \quad (17)$$

$$Bi(x) \approx \frac{1}{\sqrt{\pi}x^{1/4}} \exp(\frac{2}{3}x^{3/2}), \quad (18)$$

and on the negative axis:

$$Ai(-x) \approx \frac{1}{\sqrt{\pi}x^{1/4}} \sin(\frac{2}{3}x^{3/2} + \frac{1}{4}\pi), \quad (19)$$

$$Bi(-x) \approx \frac{1}{\sqrt{\pi}x^{1/4}} \cos(\frac{2}{3}x^{3/2} + \frac{1}{4}\pi). \quad (20)$$

At the side of positive x (negative ER), the Bi' eigenfunctions diverge exponentially in $|R|^{3/2}$, and are hence non-normalizable. On the other hand, the functions $Ai'(x)$ admit a well-behaved asymptotic behavior for both signs of R (exponential decay at one side and oscillations at the other side). Thus, the permitted eigenfunctions are

$$\psi_E(R) = Ai'(-E^{1/3}R), \quad (21)$$

yielding an unbounded, non-degenerate, continuous spectrum.

In the next section we shall construct a well-localized initial wave packet far from the singularity [14], and the far-zone asymptotic behavior of the eigenfunctions will play a key role in the construction. We introduce new variables related to R and E , in order to give this asymptotic behavior a more standard form of harmonic functions.

First we define $r(R)$ (and its inverse) to be

$$r \equiv \frac{\sqrt{2}}{3} \text{sign}(R) |R|^{3/2}, \quad R \equiv \frac{3^{2/3}}{2^{1/3}} \text{sign}(r) |r|^{2/3}. \quad (22)$$

We also define a variable k satisfying

$$E = \frac{1}{2}k^2. \quad (23)$$

We shall only use $E > 0$ eigenfunctions for the construction of our wave packet (see next section). In terms

of the new variables k, r , the $E > 0$ eigenfunctions $\psi_k(r) \equiv \psi_{E(k)}(R(r))$ read

$$\psi_k(r) = Ai'[-\text{sign}(r) |(3/2)kr|^{2/3}]. \quad (24)$$

Their far-zone asymptotic behavior becomes:

$$\psi_k(r) \approx -\frac{|(3/2)kr|^{1/6}}{\sqrt{\pi}} \cos(|k|r + \pi/4) \quad (|k|r \gg 1) \quad (25)$$

and

$$\psi_k(r) \approx -\frac{|(3/2)kr|^{1/6}}{2\sqrt{\pi}} \exp(-|k|r) \quad (|k|r \ll -1). \quad (26)$$

IV. CONSTRUCTING THE INITIAL WAVE PACKET

Next we construct a well-localized initial wave packet $\Psi_0(r) \equiv \Psi(r, t = 0)$ from the system's eigenfunctions. In the analogous free-particle problem, it is often found convenient to consider gaussian wave packets. Inspired by the harmonic form of the asymptotic behavior (25) (along with the relation $E \propto k^2$), which resembles a free particle, we shall seek an approximately-gaussian initial wave function in our problem too. This gaussian is presumably centered at some initial location $r_0 > 0$, with width δr_0 , and it propagates from large to small r with a certain averaged wave-number $k_0 < 0$. The desired fiducial gaussian is thus

$$\sim e^{i k_0 r} e^{-\frac{(r-r_0)^2}{\delta r_0^2}}. \quad (27)$$

We design our initial wave function to be sharply peaked in both r -space and k -space. Correspondingly, we demand $\delta r_0 \ll r_0$ and $\delta k \ll |k_0|$, where $\delta k \equiv 1/\delta r_0$. These inequalities (which may always be achieved by choosing sufficiently large r_0 and $|k_0|$) also imply $r_0|k_0| \gg 1$.

To accord with the above requirements, we take our initial wave function to be

$$\Psi_0(r) = \int_{-\infty}^{\infty} c(k) \psi_k(r) dk, \quad (28)$$

where

$$c(k) = \beta e^{-i r_0 \tilde{k}} e^{-\delta r_0^2 \tilde{k}^2/4}, \quad (29)$$

$\tilde{k} \equiv k - k_0$, and β is a certain normalization factor (determined below). [15] Note that $c(k)$ is just the k -th Fourier coefficient associated with the fiducial gaussian (27). Figure 1 below illustrates (for the specific case $r_0 = 4, k_0 = -40, \delta r_0 = 1/2$) that this $\Psi_0(R)$ has the desired well-localized gaussian-like shape.

We now analytically demonstrate that Eqs. (28,29), combined with the above inequalities, indeed yield an

approximate Gaussian. Since our wave packet is presumably sharply peaked in both r -space and k -space, the inequality $r_0|k_0| \gg 1$ ensures that $|k|r \gg 1$ is satisfied throughout the phase-space region which dominates $\Psi_0(r)$. We may therefore approximate the eigenfunctions $\psi_k(r)$ by their far-zone harmonic form (25). Also, in the factor $\cos(|k|r + \pi/4)$ therein we may replace $|k|$ by $-k$ to facilitate analytic integration. [16] Furthermore, in the prefactor $|(3/2)kr|^{1/6}$ we may approximate k by k_0 . We obtain the approximate asymptotic form

$$\psi_k(r) \approx \alpha|r|^{1/6} \cos(-kr + \pi/4), \quad (30)$$

where $\alpha \equiv -\pi^{-1/2}(\frac{3}{2}|k_0|)^{1/6}$. Substituting this approximate $\psi_k(r)$ in Eq. (28) and integrating over k , one obtains

$$\gamma_0|r|^{1/6} \left[e^{i k_0 r} e^{-\frac{(r-r_0)^2}{\delta r_0^2}} - i e^{-i k_0 r} e^{-\frac{(r+r_0)^2}{\delta r_0^2}} \right], \quad (31)$$

where $\gamma_0 = -\frac{(-1)^{3/4}\sqrt{\pi}}{\delta r_0} \alpha \beta$. This describes the desired gaussian at $r \sim r_0$ plus an undesired one at $r \sim -r_0$. One should recall, however, that the harmonic approximation (30) for $\psi_k(r)$ only holds for positive r (with $|k|r \gg 1$). For negative r the eigenfunctions are instead exponentially damped (by the huge factor $\exp(|k_0|r_0) \gg 1$), as seen in Eq. (26). Therefore we are only left with the desired positive- r (approximate [17]) gaussian:

$$\Psi_0(r) \approx \gamma_0|r|^{1/6} e^{i k_0 r} e^{-\frac{(r-r_0)^2}{\delta r_0^2}}. \quad (32)$$

The normalization condition $\int |\Psi_0|^2 (dR/dr) dr = 1$ now implies $\gamma_0 = \frac{3^{1/6}}{2^{1/12} \sqrt{\delta r_0} \pi^{1/4}}$, which in turn yields $\beta = -\frac{(1+i)\sqrt{\delta r_0}}{2^{5/12} \pi^{1/4} |k_0|^{1/6}}$.

Summarizing this section, our initial wave function $\Psi_0(r)$ is given by Eq. (28) combined with Eqs. (29) and (24) — which yield the desired well-localized, approximately-gaussian shape (32). Switching back from r to R we obtain

$$\Psi_0(R) = \beta \int_{-\infty}^{\infty} e^{i r_0 \bar{k} - \delta r_0^2 \bar{k}^2/4} Ai' \left[-\frac{|k|^{2/3}}{2^{1/3}} R \right] dk, \quad (33)$$

where, recall, $\tilde{k} = k - k_0$.

Figure 1 displays both the exact $\Psi_0(R)$ of Eq. (33) and its approximate form (32) (with r translated back to R), for the set of parameters $r_0 = 4$, $k_0 = -40$, and $\delta r_0 = 1/2$. The two graphs are indistinguishable, indicating the validity of the above approximations.

V. TIME EVOLUTION OF THE WAVE PACKET

The time evolution of Ψ is dictated by the Schrodinger equation (13), which endows each component ψ_k in Eq. (28) with an extra phase factor $\exp(-iEt)$:

$$\Psi(r, t) = \int_{-\infty}^{\infty} c(k) \psi_k(r) e^{-i(\frac{1}{2}k^2)t} dk. \quad (34)$$

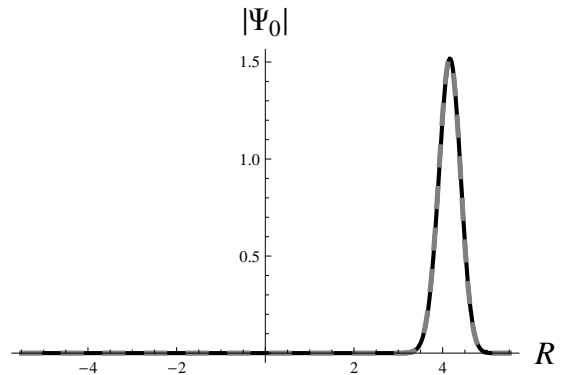


FIG. 1: The initial wave function $|\Psi_0|$ as a function of R , constructed from Eq. (33) (solid black), and compared with the approximation (32) (dashed gray). Note the non-existence of the "mirror" Gaussian on the negative side of R . Note also that $r_0 = 4$ corresponds to initial location $R = 3^{2/3}2 \approx 4.16$.

More explicitly, transforming r back to R ,

$$\Psi(R, t) = \beta \int_{-\infty}^{\infty} e^{-i(\frac{1}{2}k^2)t} e^{-i r_0 \bar{k} - \delta r_0^2 \bar{k}^2/4} Ai' \left[-\frac{|k|^{2/3}}{2^{1/3}} R \right] dk. \quad (35)$$

We shall first inspect $\Psi(R, t)$ numerically, and then explore it analytically.

Numerical evaluation

We numerically evaluated Eq. (35) for the particular case $r_0 = 4$, $k_0 = -40$, $\delta r_0 = 1/2$ (yielding $\delta k \equiv 1/\delta r_0 = 2$).

To this end we approximate the integral over k by a summation over a discrete set of equally-spaced values of k , separated by a small interval ε , in the range $k_0 - \Delta k \geq k \geq k_0 + \Delta k$. To achieve numerical precision the parameters $\varepsilon, \Delta k$ must satisfy $\varepsilon \ll \delta k$ and $e^{-(\Delta k/2\delta k)^2} \ll 1$. We choose here $\varepsilon = \delta k/20 = 0.1$ and $\Delta k = 5\delta k = 10$. The plots were insensitive to any further increase of Δk or decrease of ε . [18]

Figure 2 shows a three-dimensional plot of $\Psi(R, t)$. It clearly demonstrates how the incident gaussian bounces off $R = 0$. The time evolution roughly consists of three stages: (1) propagation from positive R toward $R = 0$, (2) the intermediate stage, near the moment of bounce, and (3) propagation of the wave packet back from the neighborhood of $R = 0$ towards large positive R . On approaching the singularity (stage 2) the wave packet develops wiggles, but subsequently it bounces and becomes nicely-peaked again (stage 3). This behavior is seen more clearly in Fig. 3, which displays a few snapshots of $\Psi(R, t)$.

We also verified numerically that the wave function preserves its unit norm upon evolution as expected. [19]

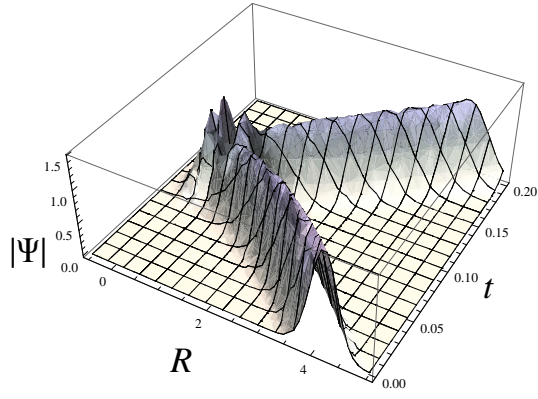


FIG. 2: A three-dimensional plot describing the time evolution of the wave function $|\Psi(R, t)|$. The bounce at $R = 0$ is evident.

A. Analytic study

Suppose that at some moment the wave function is located away from $r = 0$, in a range of r satisfying $r |k_0| \gg 1$. Then, as was discussed in the previous section, the oscillatory far-zone asymptotic behavior applies and we may represent the eigenfunctions by their approximate form (30). It is useful to define an auxiliary function $\tilde{\Psi}(r, t)$ by substituting this approximation for $\psi_k(r)$ in Eq. (34):

$$\tilde{\Psi}(r, t) \equiv \alpha |r|^{1/6} \int_{-\infty}^{\infty} c(k) e^{-i(\frac{1}{2}k^2)t} \cos(-kr + \pi/4) dk. \quad (36)$$

This function provides valuable insight into the dynamics of Ψ as we shortly demonstrate. The integration is straightforward [in fact this integral is exactly the same as the time evolution of a free Schrodinger particle with a double-gaussian initial state as in Eq. (31)]. We present $\tilde{\Psi}$ as

$$\tilde{\Psi}(r, t) = \gamma |r|^{1/6} [\Phi_- e^{ik_0 r} e^{-\frac{[r-r_c(t)]^2}{\delta r(t)^2}} + \Phi_+ e^{-ik_0 r} e^{-\frac{[r+r_c(t)]^2}{\delta r(t)^2}}], \quad (37)$$

$$\text{where } \gamma = \frac{3^{1/6}}{2^{1/12} \sqrt{\delta r(t)} \pi^{1/4}},$$

$$r_c(t) = r_0 + k_0 t, \quad (38)$$

and

$$\delta r(t) = \sqrt{\delta r_0^2 + \left(\frac{2t}{\delta r_0}\right)^2}. \quad (39)$$

Φ_- and Φ_+ are certain phase factors ($|\Phi_{\pm}| = 1$) whose explicit form will not concern us. Evidently $\tilde{\Psi}(r, t)$ is a superposition of two gaussians which propagate at opposite directions, one located at $r = r_c(t)$ and the other at $r = -r_c(t)$. Both gaussians approach $r = 0$ at time

$$t_{hit} = -\frac{r_0}{k_0}. \quad (40)$$

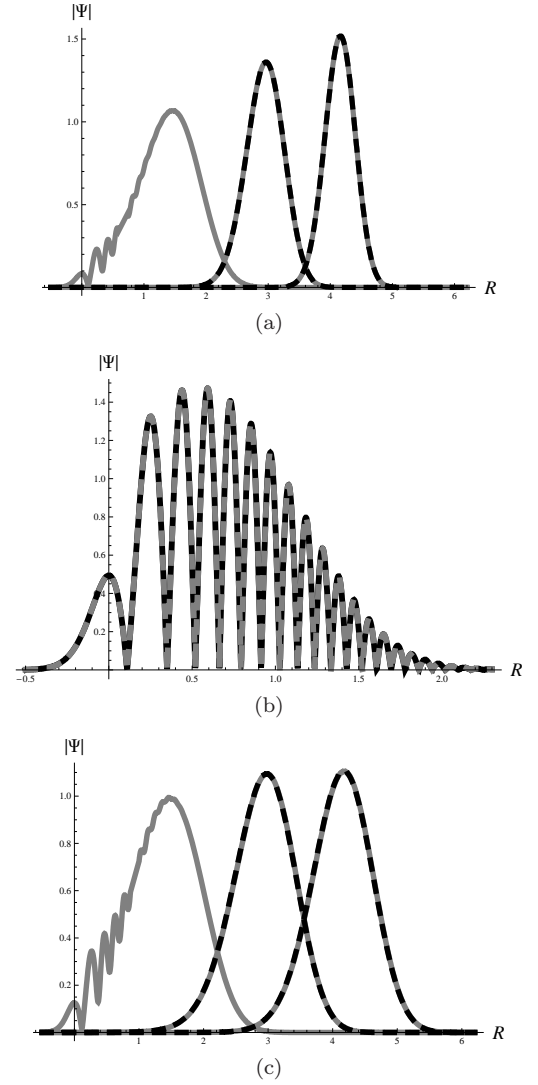


FIG. 3: Plots of $|\Psi|$ as a function of R at several different times, as it propagates towards the singularity (a), hits the singularity (b), and then recedes from it (c). The solid-gray lines and dashed-black lines represent the numerical calculations and analytic approximations, respectively. Figure 3a displays three snapshots which, going from right to left, correspond to times $t = 0, 0.04, 0.08$. Fig. 3b Displays $|\Psi|$ at $t = t_{hit} = 0.1$. Fig. 3c again displays three snapshots which, going from left to right, correspond to times $t = 0.12, 0.16, 0.2$. The analytic approximation (dashed-black line) in the two right-most graphs of both figures 3a and 3c corresponds to Eq. (41). In Fig. 3b the analytic approximation corresponds to Eq. (42).

As long as the two gaussians comprising $\tilde{\Psi}$ are remote from $r = 0$ — namely, $|r_c(t)| \gg \delta r(t)$ — the inequality $|r k_0| \gg 1$ is satisfied throughout both gaussians. Repeating the argument which led to Eq. (32) above, we find that the true wave-function Ψ will only contain the

positive- r Gaussian:

$$|\Psi(r, t)| \simeq \gamma |r|^{1/6} e^{-\frac{|r-r_c(t)|^2}{\delta r(t)^2}} \quad |r_c(t)| \gg \delta r(t). \quad (41)$$

This single-gaussian shape characterizes the wave function in both stages 1 and 3 (namely, the propagation toward $R = 0$, and back from $R = 0$ towards large positive R , respectively). It is illustrated in the two right-most graphs in both Figures 3a and 3c. These graphs display both the exact wave-function (35) and the (visually-indistinguishable) corresponding single-gaussian approximation (41). Notice that the gaussians in Fig. 3c are wider than their counterpart in Fig. 3a, which simply expresses the monotonic growth of $\delta r(t)$.

The intermediate stage 2 occurs at $t \sim t_{hit}$, when the gaussian arrives at the very neighborhood of $r = 0$. During this stage $|\Psi|$ develops numerous wiggles, as demonstrated in Fig. 3b (and also, to some extent, in the left-most graphs of Figs. 3a and 3c). Qualitatively this behavior may be interpreted as an interference pattern resulting from the overlap of the two gaussians comprising $\tilde{\Psi}$. In particular the right wings of both gaussians superpose at a range of positive r values of order a few times δr . This superposition leads to an oscillatory interference pattern in $\tilde{\Psi}$, with a typical wave-number k_0 . Since $|k_0|\delta r \gg 1$, the far-zone harmonic approximation (30) holds at $r \sim \delta r > 0$ (for both gaussians), hence $\Psi \approx \tilde{\Psi}$ in this range. [20]

This qualitative picture only yields a rough approximation for Ψ in stage 2, because near $r = 0$ the far-zone approximation breaks. However, one can show (by matching two different asymptotic approximations) that at the very moment of bounce the following approximation holds:

$$\Psi(r, t = t_{hit}) \cong \lambda e^{-qr^2} Ai'[-(k_0^2/2)^{1/3}R(r)]. \quad (42)$$

where $q = (\delta r_0^2 - 2it_0)^{-1}$ and λ is a certain coefficient. Figure 3b displays both this approximate expression and the full function $\Psi(r, t = t_{hit})$, demonstrating a nice agreement.

Finally, we comment on the quantum dynamics of the other degree of freedom Z . Since Z evolves as a free particle [See Eq. (10)] the quantum formulation adds nothing to its semiclassical dynamics: The wave-function Ψ_Z , which describes the quantum dynamics of Z , will just propagate freely, totally ignoring the $R = 0$ singularity.

VI. SEMICLASSICAL EVOLUTION BEYOND THE SINGULARITY

In both stages 1 and 3, the wave-function is sharply peaked at

$$r = |r_c(t)| = k_0|t - t_{hit}|. \quad (43)$$

By the correspondence principle, this orbit should correspond to some semiclassical solution. Indeed, translating

back from r to R , we obtain

$$R(t) = B_0|t - t_0|^{\frac{2}{3}}, \quad (44)$$

with $B_0 = |3k_0/\sqrt{2}|^{2/3}$ and $t_0 = t_{hit}$, in full consistency with Eq. (8).

One of our main goals was to obtain the semiclassical extension beyond the $R = 0$ singularity. This extension is now determined (within the near- $R = 0$ approximation) by the last formula: It is just a time-reflection of the semiclassical solution at $t < t_0$.

Note that the parameters B_0, t_0 which characterize the extension at $t > t_0$ are fully determined by the semiclassical evolution at $t < t_0$. In particular, in Ref. [5] it was found that for a macroscopic ($M \gg K$) CGHS black hole $B_0 \approx [(3/2)\sqrt{K}M]^{2/3}$, where M denotes the (remaining) black-hole mass.

The other degree of freedom Z just evolves steadily at $t \sim t_0$ (at the leading order); Namely,

$$Z(t) \simeq z_0 + z_1(t - t_0), \quad (45)$$

where z_0, z_1 are constants which are again determined by the semiclassical evolution at $t < t_0$.

Note that the extension (44), which satisfies $B(t > t_0) = B(t < t_0)$, is the only one which conserves H across the singularity, as may be seen from Eq. (12) (which holds at both $t < t_0$ and $t > t_0$).

It should be emphasized that the exact time-reflection symmetry exhibited in Eq. (44) only characterizes the *leading-order* semiclassical evolution near $R = 0$. Beyond the leading order R and Z do couple [as may be seen, for example, by substituting $S = (Z - \tilde{R})/K$ in Eq. (5)], which spoils the time-reflection symmetry of $R(t)$. The semiclassical evolution at $t > t_0$ *beyond* the leading order may be obtained by taking Eq. (44) and the above linear expression for $Z(t)$, translated back to \tilde{R} and S , as initial conditions for the full system (5,6).

VII. DISCUSSION

It is a common belief that Quantum Gravity will eventually cure the spacetime singularities, which are known to occur in classical and semiclassical gravitational collapse (as well as in cosmology). Here we demonstrated this idea by applying a simplified quantization procedure to the spacelike $R = 0$ singularity inside a two-dimensional CGHS [3] evaporating BH. This allows us to explore the extension of spacetime physics beyond the singularity.

Our quantization procedure is based on the minisuperspace approach, in which all degrees of freedom associated with inhomogeneities are erased. The system's evolution is then described by a wave-function, whose time evolution is dictated by a Schrodinger-like equation, which we solve analytically.

Our most crucial observation is that *quantum evolution is perfectly regular (in fact, analytic) across the*

semiclassical $R = 0$ singularity. (This is far from obvious, because the Hamiltonian operator itself is singular at $R = 0$.) This analyticity gives rise to unique quantum evolution across the singularity. We find that an initially-localized wave packet spreads and fluctuates on approaching $R = 0$, but then it bounces back toward positive R values. This is demonstrated in Figs. 2 and 3. Following the bounce, the wave packet becomes sharply-peaked again, and approaches a well-defined semiclassical orbit.

The main objective of this paper was to explore the extension of spacetime physics beyond the $R = 0$ singularity inside the BH. The wave-packet dynamics described above indicates that the strong quantum fluctuations which develop at the very neighborhood of $R = 0$ quickly die out, giving rise to a new semiclassical phase beyond the singularity. The quantum dynamics also determines the structure of spacetime (namely, the spacetime dependence of the two semiclassical variables R and Z) in this new patch, by dictating the boundary conditions for R and Z across the singularity: First, both variables are continuous. Second, R bounces there at a (locally) time-symmetric manner, whereas Z evolves steadily across the singularity. These boundary data for both R , Z and their time derivative (which in fact amount to specifying the parameters B_0, t_0, z_0, z_1 of Sec. VI) give rise to a unique and well-defined semiclassical Cauchy evolution at the future side of the spacelike singularity, the region denoted by D in Fig. 4

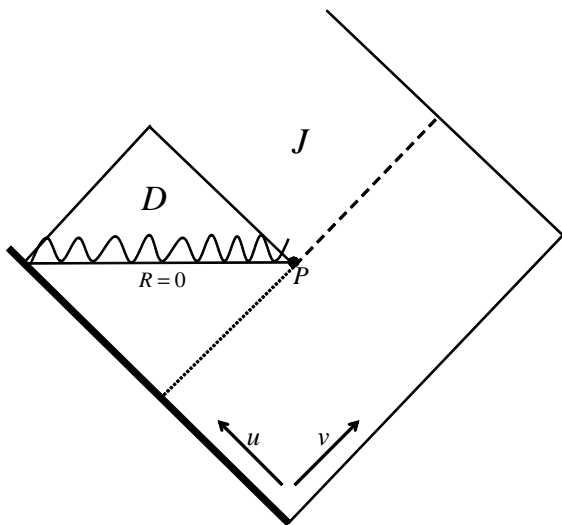


FIG. 4: Spacetime diagram of a CGHS black hole which forms by gravitational collapse and subsequently evaporates. The thick null line at the bottom left represents the collapsing massive shell. The event horizon is marked by a dotted line. D represents the future Cauchy development of the singularity line $R = 0$. The domain marked by J is discussed in the text.

Interestingly, the situation found here resembles the recent developments in Loop Quantum Cosmology (LQC) in many respects. Several analyses showed that in various homogeneous cosmological models (open or closed

universe, with or without cosmological constant) the classical big-bang singularity is replaced in LQG by a regular bounce. [9] The same behavior (quantum singularity resolution, and a consequent bounce) was obtained here in a two-dimensional BH—though within a more simplified quantum formulation. There appears to be an important difference, though: In our case the very epoch of bounce is marked by strong quantum fluctuations, whereas the cosmological bounce in LQC is typically free of such strong fluctuations.

An obvious extension of this research is to obtain the specific structure of semiclassical spacetime [namely, the functions $R(u, v)$ and $S(u, v)$] beyond the singularity. In the present work we obtained the required boundary data for these functions at the future side of the singularity. The calculation of post-singular $R(u, v)$ and $S(u, v)$ may naturally be divided into three stages: (i) The asymptotic behavior in the very neighborhood of the singularity is already given in Eqs. (44) and (45). It applies as long as $R \ll K$. [21] (ii) In an intermediate stage of larger $t - t_0$ values, these simple asymptotic expressions no longer hold. Furthermore, R and Z no longer evolve independently. Still (as long as $t - t_0 \ll M/K$) the homogeneous approximation applies, and the evolution of $R(t)$ and $S(t)$ is determined by the ordinary differential equations (5,6). (iii) For even larger values of $t - t_0$, the large-scale inhomogeneous character of spacetime comes into expression, and the evolution of $R(u, v)$ and $S(u, v)$ must be determined by evolving the partial differential equations (4). In both stages (ii) and (iii), the evolution can be analyzed either numerically or by certain analytic approximations (which are beyond the scope of the present paper). A numerical simulation of the semiclassical CGHS field equations is underway [10, 11], and perhaps it will be possible to extend this numerics to the post-singularity region as well. By this way it should be possible to determine the semiclassical spacetime [particularly the functions $R(u, v)$ and $S(u, v)$] in the entire future "domain of dependence" of the spacelike line $R = 0$, the triangle-like region denoted by D [which is actually $D_+(R = 0)$] in Fig. 4.

Note, however, that after the structure of the domain $D_+(R = 0)$ is exposed, one will still face the most challenging stage in the task of composing the overall post-singularity semiclassical spacetime: Revealing spacetime physics in the "wedge" between $D_+(R = 0)$ and the external asymptotically-flat region (the domain denoted J in Fig. 4). A priori it is not even clear if this "piece" is connected (as suggested by the ATV point of view [8], which assumes a fiducial Minkowskian \mathcal{R}^2 manifold) or disconnected (as may be suggested by the more common paradigm, see e.g. Fig. 5 in Ref. [2]). It seems that new concepts and insights will be needed in order to explore this remaining piece of the puzzle.

VIII. ACKNOWLEDGEMENTS

We would like to thank Joseph Avron, Oded Kenneth, Martin Fraas, and Joshua Feinberg for helpful discussions. We are especially grateful to Abhay Ashtekar for

warm hospitality, for his advice and encouragement and for many fruitful discussions. This research was supported in part by the Israel Science Foundation (grant no. 1346/07).

-
- [1] See Sec. 8.2 in *The Large Scale Structure of Space-Time* S. W. Hawking and G. F. Ellis (Cambridge university press 1973).
- [2] S. W. Hawking, *Commun. Math. Phys.* **43**, 199 (1975).
- [3] C. G. Callan, S. B. Giddings, J.A. Harvey and A. Strominger, *Phys. Rev.* **D45**, R1005 (1992).
- [4] J. G. Russo, L. Susskind and L. Thorlacius, *Phys. Lett.* **B292**, 13 (1992).
- [5] D. Levanony and A. Ori, *Phys. Rev.* **D80**, 084008 (2009).
- [6] J. Tipler, *Phys. Lett.* **64a**, 8 (1977)
- [7] See also A. Ori, *Phys. Rev. D.* **61** 064016 (2000).
- [8] A. Ashtekar, V. Taveras, and M. Varadarajan, *Phys.Rev.Lett.***100**, 211302 (2008).
- [9] E. Bentivegna and T. Pawłowski, *Phys. Rev.* **D77**, 124025 (2008); A. Ashtekar, T. Pawłowski, P. Singh and K. Vandersloot, *Phys. Rev.* **D75**, 024035 (2007); A. Ashtekar, T. Pawłowski and P. Singh, *Phys. Rev. Lett.* **96**, 141301 (2006); A. Ashtekar, *Gen. Rel. and Grav.* **41** 707 (2009) and references therein.
- [10] L. Dori, research in progress
- [11] E. M. Ramazanoglu and F. Pretorius, research in progress.
- [12] As was already mentioned above, our effective Hamiltonian H is determined at the semiclassical level up to an arbitrary multiplicative constant. Changing this constant will also result in a rescaling of E and of the time-scale for quantum evolution.
- [13] For negative E , by $E^{(1/3)}$ we actually refer to the real branch $-|E|^{(1/3)}$. Note also that for $E = 0$ the solution is trivial, $\psi_{E=0}(R) = C_1 + C_2 R^2$. However, since the spectrum is continuous, the single exceptional eigenvalue $E = 0$ will have no special significance.
- [14] By "far from the singularity" we mean that the wave-packet distance (in R) from the singularity is much larger than its width (namely, $r_0 \gg \delta r_0$ in the notation introduced below). Yet, as explained in Secs. I and II, the region of spacetime addressed in this paper is the asymptotic region near the singularity, namely $|R| \ll K$. These two assumptions do not conflict, provided that $\delta r_0 \ll K$.
- [15] In constructing this $\Psi_0(R)$ we have only used $E > 0$ modes. Note that the modes of negative E oscillate at $r < 0$ but decay exponentially at $r > 0$. These modes are inappropriate for representing our initial wave packet, which is required to be sharply peaked at positive $r \sim r_0$.
- [16] This leads to a negligible error because for all eigenfunctions with $k > 0$, $c(k)$ is suppressed by the factor $\exp[(k_0 \delta r_0/2)^2] \gg 1$.
- [17] Note that over the narrow gaussian (recall $\delta r_0 \ll r_0$), the factor $|r|^{1/6}$ may be approximated as a constant, and we may therefore refer to Eq. (32) as an approximate gaussian. The same applies to the moving gaussian of $\Psi(r, t)$ (in stages 1 and 3), considered in Sec. V .
- [18] Changing from integration over k to sum over a discreet set of k values results in an infinite sequence of spurious replica gaussians, with r -separation that scales as $1/\varepsilon$ (like in standard Fourier decomposition). Our ε is sufficiently small that all spurious copies are well separated and do not interfere with the authentic function Ψ that we display.
- [19] Over the time range covered by Fig. 3, the norm was numerically found to vary by less than 10^{-3} .
- [20] On the other hand, the $r < 0$ portion of the interference pattern will not be realized in Ψ , due to the exponential decay in the corresponding far-zone asymptotic behavior (26).
- [21] In considering this stage of evolution [as well as stage (ii) below], one should bear in mind that the approximate homogeneity of the singularity only holds at spatial scales that are short compared to the evaporation time scale. When considering the overall large-scale post-singularity evolution, one should regard the matching "parameters" B_0, t_0, z_0, z_1 as functions of v which slowly drift along the line of singularity (just like the effective local mass M). These four functions may be obtained by evolving the CGHS field equations from the initial data up to the (past side of the) singularity.